Brane order, quantum magnetism, and partition function zeros in modulated anisotropic ladders

Gennady Y. Chitov
Département de physique
Université de Sherbrooke
Québec, Canada

Talk in the Landau Institute for Theoretical Physics, April 21, 2023

PHYSICAL REVIEW B **106**, 094413 (2022)

Brane order and quantum magnetism in modulated anisotropic ladders

Toplal Pandey[1] and Gennady Y. Chitov[2]
[1]*Department of Physics, Laurentian University, Sudbury, Ontario, P3E 2C6 Canada*
[2]*Institut quantique & Département de physique, Université de Sherbrooke, Sherbrooke, Québec, J1K 2R1 Canada*

Research supported by:
Institut Quantique (IQ) of U. de Sherbrooke
Reseau Quebecois des Materiaux de Pointe (RQMP)

INSTITUT QUANTIQUE
UNIVERSITÉ DE SHERBROOKE

RQMP

Outline:

- *Formulation of the main problem*
- *Model of the dimerized XYZ ladders*
- *Methods and approximations*
- *Brane order parameters, dualities, SSB*
- *Lee-Yang zeros: topological numbers, Majorana modes, disorder lines and disentanglement*
- *Experiments to detect the brane order*
- *Discussion of other papers pertinent to the thesis*

Landau Framework (Paradigm):

E.g., Chaikin, Lubensky

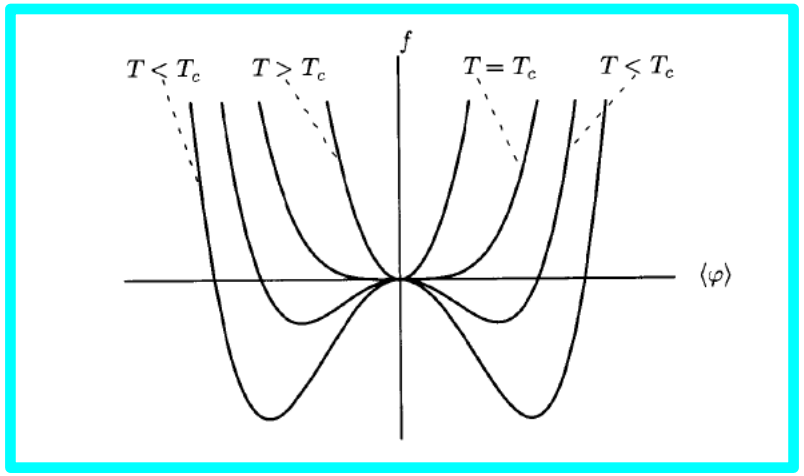

Spontaneous Symmetry Breaking

$$f(T,\langle\phi\rangle) = \frac{1}{2}r\langle\phi\rangle^2 + u\langle\phi\rangle^4, \qquad r = a(T - T_c).$$

$$\langle\phi\rangle = \begin{cases} 0 & \text{if } T > T_c; \\ \pm(-r/4u)^{1/2} & \text{if } T < T_c. \end{cases}$$

$$\langle\phi\rangle \sim (T_c - T)^{\beta}, \qquad \beta = 1/2.$$

$$\chi \sim |T - T_c|^{-\gamma}, \qquad \gamma = 1.$$

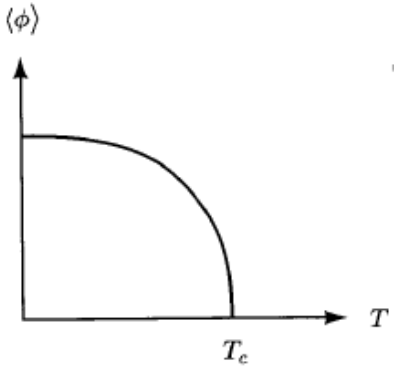

Order parameter: magnetization, density, lattice displacement, superconducting wave function, etc.

Landau Paradigm, refined, beyond mean field:

Table 5.4.1. *Definition of critical exponents and amplitudes.*

Susceptibility	$\chi = \Gamma t^{-\gamma}$	$t > 0$
	$\chi = \Gamma'(-t)^{-\gamma'}$	$t < 0$
Specific heat	$C = \frac{A}{\alpha} t^{-\alpha}$	$t > 0$
	$C = \frac{A'}{\alpha'}(-t)^{-\alpha'}$	$t < 0$
Correlation length	$\xi = \xi_0 t^{-\nu}$	$t > 0$
	$\xi = \xi_0'(-t)^{-\nu'}$	$t < 0$
Order parameter	$\langle \phi \rangle = B(-t)^{\beta}$	$t < 0$
	$\langle \phi \rangle = D_c^{-1} h \lvert h \rvert^{(1-\delta)/\delta}$	$t = 0$
Correlation function	$G(q) = D_\infty q^{-(2-\eta)}$	$t = 0$

Universality

Scaling Relations

$$\gamma = (2 - \eta)\nu$$

$$\gamma + 2\beta = d\nu.$$

Example: 2D Ising Model

$\alpha = 0,\ \beta = 1/8,\ \nu = 1,\ \eta = 1/4$

Not so fast!!!

Examples:

Fractional Quantum Hall Effect (FQHE)

Mott insulators

Topological insulators

Spin and Majorana chains/ladders

Kitaev-Heisenberg materials

HUGE (!!!) literature

E.g.,

X.-G. Wen, Rev. Mod. Phys. 89, 041004 (2017);

Bei Zeng, Xie Chen, Duan-Lu Zhou, Xiao-Gang Wen, *Quantum Information Meets Quantum Matter – From Quantum Entanglement to Topological Phase in Many-Body Systems,* Springer (2019).

Fundamental difficulties: Order parameter, Symmetry breaking

The augmented Landau framework (paradigm):

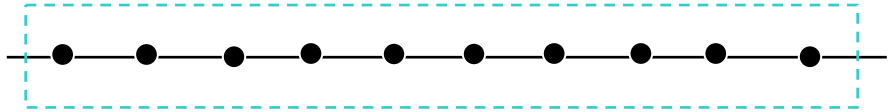

N-string

$\prod_{i=1}^{N} Q_n$

Refs: den Nijs and Rommelse, PRB (89)
Berg, Giamarchi, et al, PRB (08)
Chen, Nussinov, J. Phys. A (08)
Montorsi, et al, PRB (16)

Strings and branes

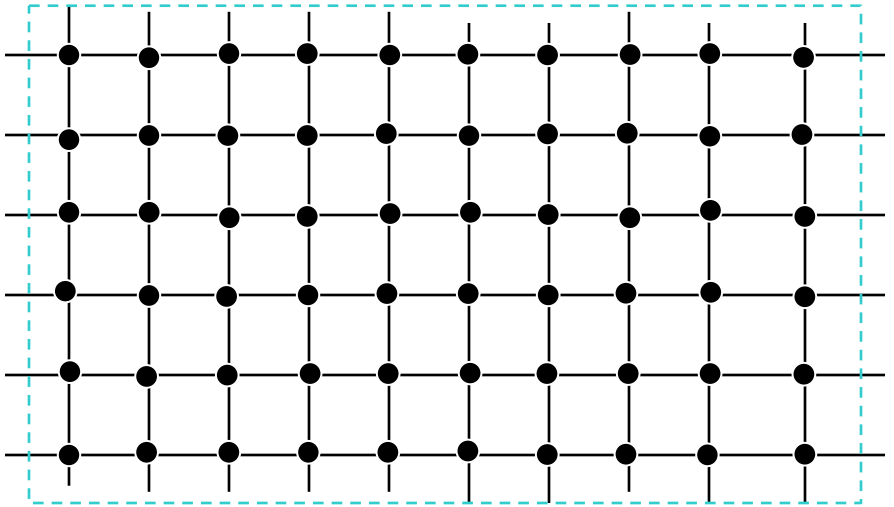

NxM-brane

$\prod_{i=1}^{N} \prod_{j=1}^{M} Q_{i,j}$

$N,M \to \infty$

Compare to two-point correlators (local order parameters)

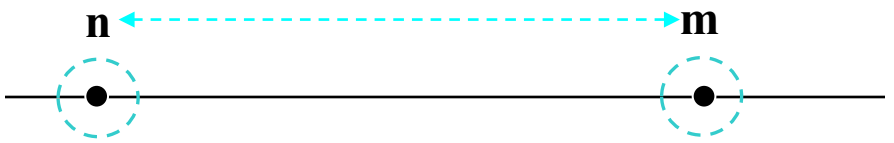

$Q_n\, Q_m$

$|m-n| \to \infty$

Order parameters: Unifying properties

Order Parameter (local): magnetization, density, lattice displacement, superconducting wave function, etc.

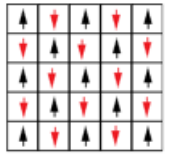

Non-local Order Parameter: string, brane parameters

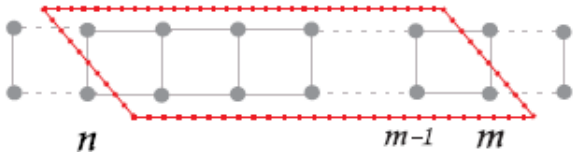

Duality Transformation maps onto some dual local order parameter

Modulated anisotropic 2-leg ladder:

Results for this pattern will be discussed

$$H = \sum_{n=1}^{N}\sum_{\alpha=1}^{2}\Big\{J_\alpha(n)\mathbf{S}_\alpha(n)\cdot\mathbf{S}_\alpha(n+1) + J\gamma\left[S^x_\alpha(n)S^x_\alpha(n+1) - S^y_\alpha(n)S^y_\alpha(n+1)\right]\Big\} + J_\perp\sum_{n=1}^{N}\mathbf{S}_\alpha(n)\cdot\mathbf{S}_{\alpha+1}(n).$$

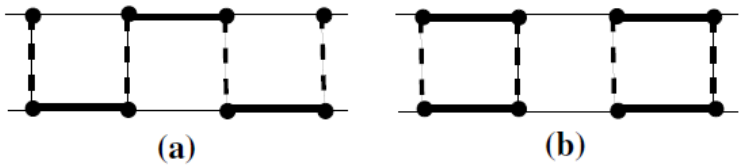

FIG. 1. Dimerized two-leg ladder. Bold or thin lines represent the stronger or weaker chain coupling; dashed lines represent rung coupling $J_\perp$, respectively. Dimerization patterns: (a) - staggered; (b)- columnar.

The two possible dimerization patterns shown in Fig. 1 are defined as:

$$J_\alpha(n) = \begin{cases} J[1+(-1)^{n+\alpha}\delta], & \text{staggered} \\ J[1+(-1)^{n}\delta]. & \text{columnar} \end{cases} \qquad (2)$$

Jordan-Wigner Transformation + Mean-field Approximation

$$H_{MF} = \frac{1}{2}\sum_n\Big\{\sum_\alpha(-1)^{n+\alpha-1}\left[J_{\alpha R}(n)c^\dagger_\alpha(n)c_\alpha(n+1) + \Gamma_R(n)c^\dagger_\alpha(n)c^\dagger_\alpha(n+1)\right] + J_{\perp R}(n)c^\dagger_1(n)c_2(n) + h.c.\Big\}$$

Staggered isotropic 2-leg ladder:

$$H = \sum_{n=1}^{N}\sum_{\alpha=1}^{m} J_\alpha(n)\mathbf{S}_\alpha(n)\cdot\mathbf{S}_\alpha(n+1) + J_\perp \sum_{n=1}^{N}\sum_{\alpha=1}^{m-1}\mathbf{S}_\alpha(n)\cdot\mathbf{S}_{\alpha+1}(n),$$

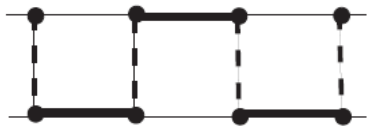

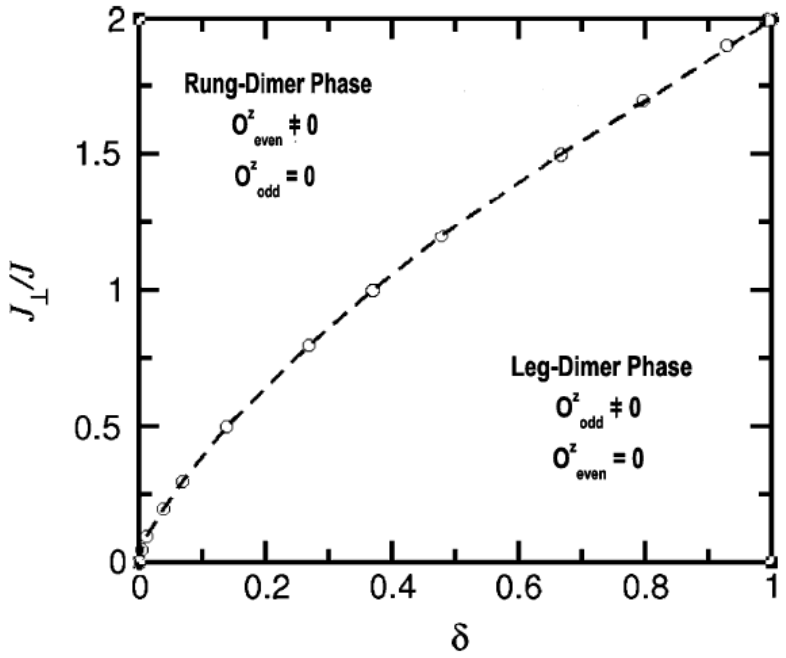

FIG. 4. Two-leg ladder; critical line $J_{\perp c}(\delta)$ where the gap of the staggered phase vanishes. Adapted from Ref. 12, original data from Ref. 9.

SANDRA J. GIBSON, R. MEYER, AND GENNADY Y. CHITOV
PHYSICAL REVIEW B **83**, 104423 (2011)

CHITOV, RAMAKKO, AND AZZOUZ
PHYSICAL REVIEW B **77**, 224433 (2008)

M. A. Martin-Delgado, R. Shankar, and G. Sierra, Phys. Rev. Lett. **77**, 3443 (1996).

See more refs on this model in PRB (2011)

Jordan-Wigner Transformation + Mean-field Approximation: Technical details

$$H = \sum_{n=1}^{N}\sum_{\alpha=1}^{2}\Big\{J_\alpha(n)\mathbf{S}_\alpha(n)\cdot\mathbf{S}_\alpha(n+1) + J\gamma\left[S^x_\alpha(n)S^x_\alpha(n+1) - S^y_\alpha(n)S^y_\alpha(n+1)\right]\Big\} + J_\perp\sum_{n=1}^{N}\mathbf{S}_\alpha(n)\cdot\mathbf{S}_{\alpha+1}(n).$$

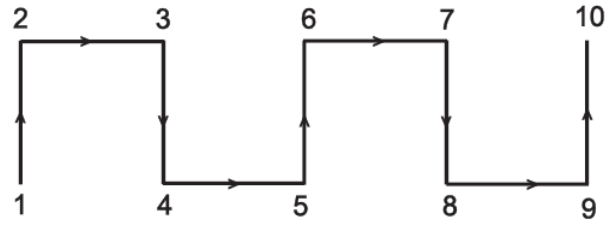

FIG. 2. The path of Jordan-Wigner transformation used for fermionization of the two-leg ladder. This is also the path used to map the sites of the two-leg ladder onto a snake-like chain.

$$\sigma_n^+ = c_n^\dagger \exp\left(\mathrm{i}\pi\sum_{l=1}^{n-1} c_l^\dagger c_l\right)$$

$$\sigma_n^z = 2c_n^\dagger c_n - 1,$$

where $\sigma_n^\pm = \frac{1}{2}(\sigma_n^x \pm \mathrm{i}\sigma_n^y)$

$$H = \frac{1}{2}\sum_{n,\alpha}\left\{e^{i\hat{\Phi}_\alpha(n)}\left(J_\alpha(n)c_\alpha^\dagger(n)c_\alpha(n+1) + \frac{J\gamma}{2}c_\alpha^\dagger(n)c_\alpha^\dagger(n+1)\right) + 2J_\alpha(n)\left(\hat{n}_\alpha(n)-\frac{1}{2}\right)\left(\hat{n}_\alpha(n+1)-\frac{1}{2}\right)\right\}$$
$$+\frac{1}{2}\sum_{n}\left\{J_\perp(n)c_1^\dagger(n)c_2(n) + 2J_\perp(n)\left(\hat{n}_1(n)-\frac{1}{2}\right)\left(\hat{n}_2(n)-\frac{1}{2}\right)\right\} + \mathrm{H.c.}$$

$$\hat{\Phi}_\alpha(m) = \begin{cases} 0 & \alpha=1,\ m=2l \\ \pi(\hat{n}_2(m)+\hat{n}_2(m+1)) & \alpha=1,\ m=2l-1 \\ 0 & \alpha=2,\ m=2l-1 \\ \pi(\hat{n}_1(m)+\hat{n}_1(m+1)) & \alpha=2,\ m=2l \end{cases}$$

According to the Lieb theorem the ground state of a quadratic fermionic Hamiltonian on a bipartite lattice at half-filling is the π-flux phase. Imposing this requirement on the approximate Hamiltonian above amounts to the approximation:

$$e^{i\hat{\Phi}_\alpha(n)} \approx (-1)^{n+\alpha-1}$$

The Hartee-Fock approximation for the fermionic interacting term:

$$\hat{n}_l\hat{n}_m \approx \tfrac{1}{2}\hat{n}_l + \tfrac{1}{2}\hat{n}_m - \tfrac{1}{4} + c_l^\dagger c_m\langle c_l c_m^\dagger\rangle + \text{H.c.} + |\langle c_l c_m^\dagger\rangle|^2 + c_l^\dagger c_m^\dagger\langle c_m c_l\rangle + \text{H.c.} - |\langle c_l c_m\rangle|^2$$

We introduce the mean-field averaged parameters:

$$t_\alpha(n) = \begin{cases} \mathcal{K} + (-1)^{n+\alpha}\delta\eta, & \text{(staggered)} \\ \mathcal{K} + (-1)^n\delta\eta, & \text{(columnar)} \end{cases},$$

$$P_\alpha(n) = \begin{cases} P - (-1)^{n+\alpha}\delta\eta_p, & \text{(staggered)} \\ P - (-1)^n\delta\eta_p, & \text{(columnar)} \end{cases}.$$

and the renormalized couplings:

$$J_{\alpha R}(n) = \begin{cases} J[t_R + (-1)^{n+\alpha}\delta_R], & \text{staggered} \\ J[t_R + (-1)^n\delta_R], & \text{columnar} \end{cases},$$

$$\Gamma_{\alpha R}(n) = \begin{cases} J[\gamma_R + (-1)^{n+\alpha}\gamma_{aR}], & \text{staggered} \\ J[\gamma_R + (-1)^n\gamma_{aR}], & \text{columnar} \end{cases},$$

$$J_{\perp R}(n) = J_\perp(1 + 2t_\perp),$$

$$t_R = 1 + 2(\mathcal{K} + \delta^2\eta),$$

$$\delta_R = \delta(1 + 2(\mathcal{K} + \eta)),$$

$$\gamma_R = \gamma - 2(P - \delta^2\eta_p),$$

$$\gamma_{aR} = -2\delta(P - \eta_p).$$

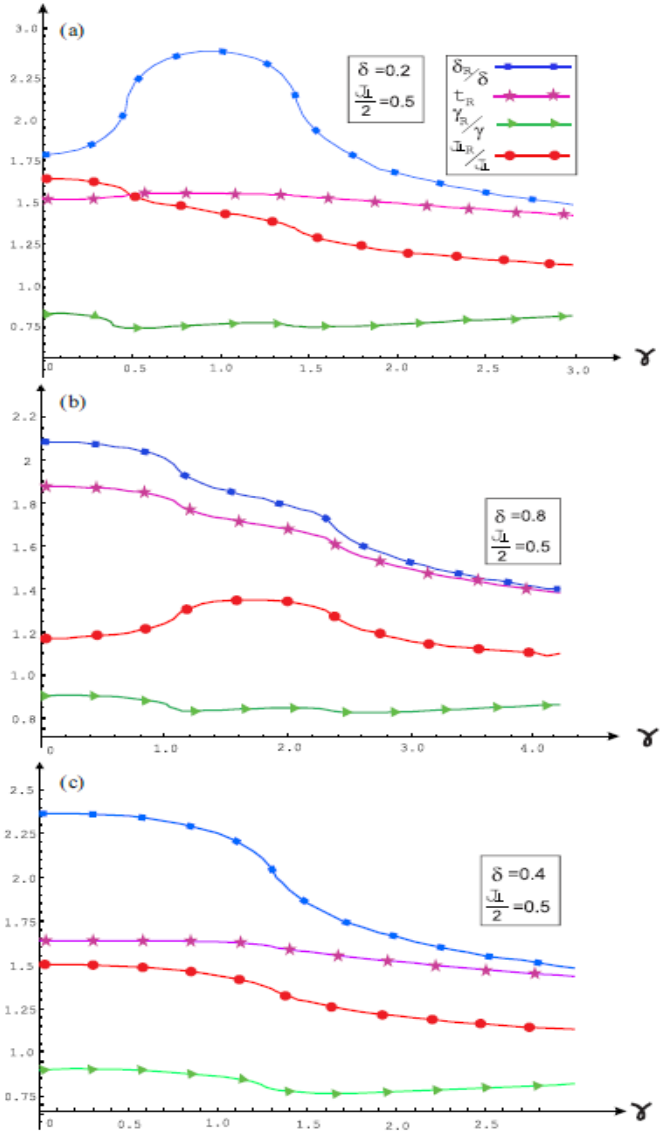

FIG. 8. The ratios of the renormalized couplings with respect to their bare values calculated from the mean-field equations. The parameters are calculated along two paths of constant δ for the staggered ladder [(a) and (b)] and one path of constant δ for the columnar ladder (c). The paths resemble those shown in Figs. 3 and 4, but taken on the plane of bare parameters (δ, γ).

Jordan-Wigner Transformation + Mean-field Approximation: Effective mean-field Hamiltonian

$$H = \sum_{n=1}^{N} \sum_{\alpha=1}^{2} \Big\{ J_\alpha(n) \mathbf{S}_\alpha(n) \cdot \mathbf{S}_\alpha(n+1) + J\gamma \big[S_\alpha^x(n) S_\alpha^x(n+1) - S_\alpha^y(n) S_\alpha^y(n+1) \big] \Big\} + J_\perp \sum_{n=1}^{N} \mathbf{S}_\alpha(n) \cdot \mathbf{S}_{\alpha+1}(n).$$

$$H_{MF} = \frac{1}{2} \sum_n \Big\{ \sum_\alpha (-1)^{n+\alpha-1} \big[J_{\alpha R}(n) c_\alpha^\dagger(n) c_\alpha(n+1) + \Gamma_R(n) c_\alpha^\dagger(n) c_\alpha^\dagger(n+1) \big] + J_{\perp R}(n) c_1^\dagger(n) c_2(n) + h.c. \Big\}$$

Staggered ladder:

The Hamiltonian matrix has four eigenvalues:

$$E_{\pm\pm}(k) = \sqrt{(\gamma_a \pm t)^2 \cos^2 k + \left((\gamma \pm \delta)\sin k \pm \frac{J_\perp}{2}\right)^2}.$$

The model is gapped in general, however the gap

$$\Delta = \left|(\gamma \pm \delta) \pm \frac{J_\perp}{2}\right|$$

vanishes on the lines of quantum critical transitions shown in Fig. 3:

$$\gamma = \pm\left|\delta \pm \frac{J_\perp}{2}\right|,$$

In terms of the Majorana operators:

$$2c^\dagger_{2n} = a_{2n} + ib_{2n-1}$$

$$H_{\rm MF} = H_o + H_e,$$

$$H_o = \frac{i}{4}\sum_{l=1}^{N}\{-(t-\gamma-\delta)b_{2l+1}a_{2l-1} + (t+\gamma+\delta)b_{2l-1}a_{2l+1} + J_\perp b_{2l-1}a_{2l-1}\},$$

$$H_e = \frac{i}{4}\sum_{l=1}^{N}\{-(t+\gamma-\delta)b_{2l-2}a_{2l+2} + (t-\gamma+\delta)b_{2l}a_{2l} + J_\perp b_{2l-2}a_{2l}\}.$$

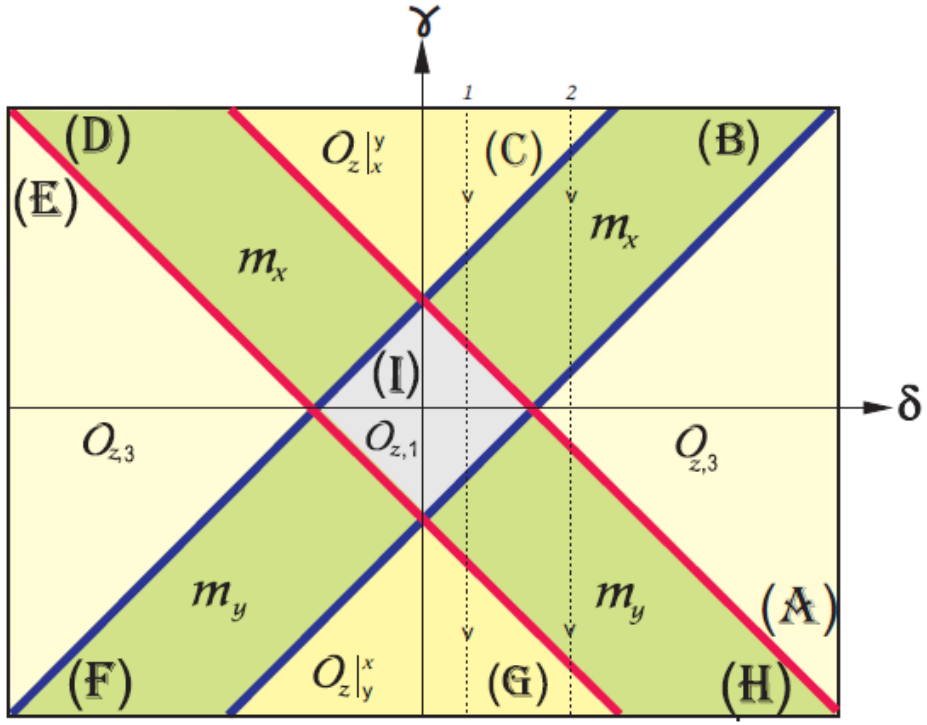

FIG. 3. Phase diagram of the anisotropic staggered two-leg ladder. Non-vanishing brane and local order parameters are shown in nine regions from A to I of the (δ, γ) parametric plane. The blue/red lines $\gamma = \pm(\delta \pm \frac{1}{2}J_\perp)$ are the lines of quantum phase transitions (gaplessness).

Majorana Hamiltonian ⟶ Inverse Jordan-Wigner Transformation + canonical transformations

The Hamiltonian maps onto two decoupled XY chains in staggered transverse field:

$$H_{\mathrm{MF}} = H_o + H_e,$$

$Z_2 \otimes Z_2$ symmetry

$$H_o = \frac{1}{4}\sum_{l=1}^{N}\{(t+\gamma+\delta)\tau_{2l-1}^{x}\tau_{2l+1}^{x} + (t-\gamma-\delta)\tau_{2l-1}^{y}\tau_{2l+1}^{y} + (-1)^{l}J_{\perp}\tau_{2l-1}^{z}\}.$$

$$H_e = \frac{1}{4}\sum_{l=1}^{N}\{(t+\gamma-\delta)\mu_{2l-2}^{x}\mu_{2l}^{x} + (t-\gamma+\delta)\mu_{2l-2}^{y}\mu_{2l}^{y} + (-1)^{l}J_{\perp}\mu_{2l-2}^{z}\}.$$

Spontaneous Symmetry Breaking

Brane Operators:

$$\mathcal{B}^i_e(n) \equiv \prod_{\alpha=1}^{2} \prod_{l=1}^{n} \sigma^i_\alpha(l), \quad i = x, y, z$$

$$\mathcal{B}^i_{o,\alpha}(n) \equiv \mathcal{B}^i_e(n-1)\sigma^i_\alpha(n), \quad \alpha = 1, 2.$$

Brane-Brane Correlation Functions:

We also define the corresponding brane-brane correlation functions which are calculated in the following: the even-even correlator

$$\langle \mathcal{B}^i_e(m)\mathcal{B}^i_e(n)\rangle \ ,$$

the mixed correlators

$$\langle \mathcal{B}^i_e(m)\mathcal{B}^i_{o,\alpha}(n)\rangle \quad \text{and } e \leftrightarrow o \ ,$$

and the odd-odd correlation function

$$\langle \mathcal{B}^i_{o,\alpha}(m)\mathcal{B}^i_{o,\beta}(n)\rangle \ .$$

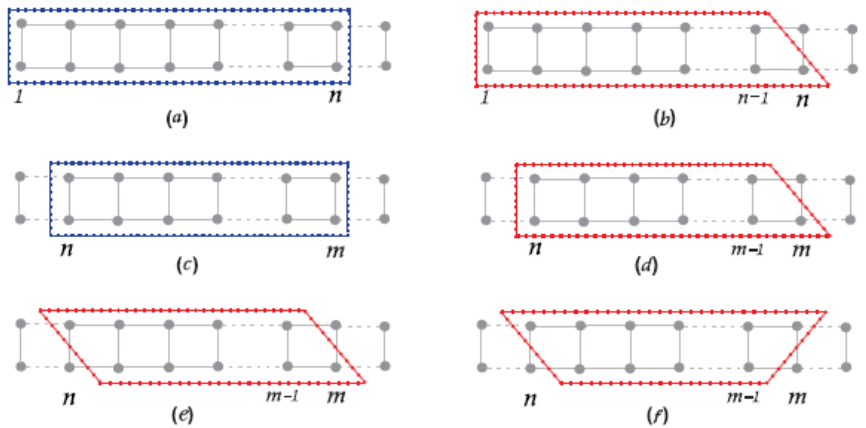

FIG. 5. Branes and brane-brane correlation functions: (a) and (b) depict an even/odd brane, resp., for (b) another odd brane may be obtained by reflection with respect to horizontal axis; (c) – even-even brane correlator; (d) – even-odd brane correlator; (e), (f) – odd-odd brane correlators. The odd-even and odd-odd brane correlators can also correspond to other graphs obtained form the cases (d-f) by reflections with respect to horizontal/vertical axes.

After relabeling ladder's sites according to the path shown in Fig. 2, the brane operators can be represented via string operators defined along a given path (say P) as

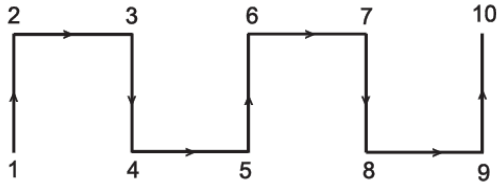

$$O_i(n) \equiv \prod_{l \leqslant n, l \in \mathcal{P}} \sigma_l^i, \quad i = x, y, z.$$

and

$$D_{ii}(L, R) \equiv O_i(L-1) O_i(R)$$

such that its average yields the string-string correlation function

$$\mathfrak{D}_{ii}(L, R) \equiv \langle D_{ii}(L, R) \rangle.$$

Region (A).

$$\tau_1^x \tau_{2N+1}^x = D_{xx}(2, 2N+1), \qquad \langle \tau_1^x \tau_{2N+1}^x \rangle \overset{[N\to\infty]}{\longmapsto} \langle \tau_x \rangle^2 = \frac{2\sqrt{t}}{t+\gamma+\delta}\left[(\gamma+\delta)^2 - \frac{J_\perp^2}{4}\right]^{1/4},$$

$$\mu_0^y \mu_{2N}^y = D_{yy}(2, 2N+1), \qquad \langle \mu_0^y \mu_{2N}^y \rangle \overset{[N\to\infty]}{\longmapsto} \langle \mu_y \rangle^2 = \frac{2\sqrt{t}}{t+|\gamma-\delta|}\left[(\gamma-\delta)^2 - \frac{J_\perp^2}{4}\right]^{1/4}$$

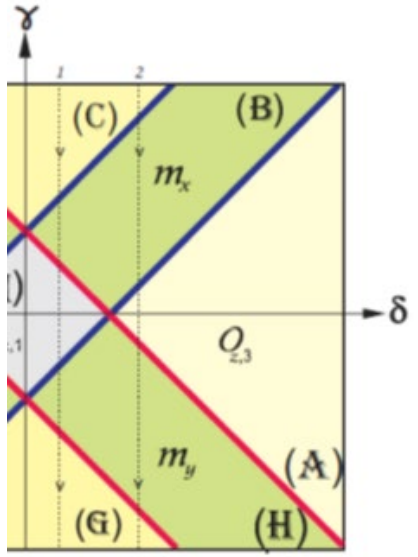

$$\langle \tau_1^x \tau_{2N+1}^x \mu_0^y \mu_{2N}^y \rangle = (-1)^N \mathfrak{D}_{zz}(2, 2N+1) \overset{[N\to\infty]}{\longmapsto} \pm \mathcal{O}_{z,3}^2,$$

$$\mathcal{O}_{z,3} = \langle \tau_x \rangle \langle \mu_y \rangle. \qquad \mathfrak{D}_{zz} \leftrightarrows \langle \mathcal{B}_{o,\alpha}^z \mathcal{B}_{o,\beta}^z \rangle$$

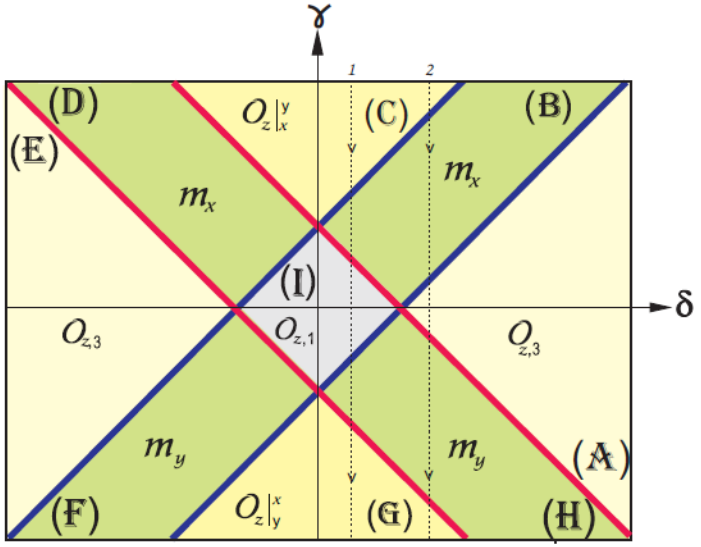

FIG. 3. Phase diagram of the anisotropic staggered two-leg ladder. Non-vanishing brane and local order parameters are shown in nine regions from A to I of the (δ, γ) parametric plane. The blue/red lines $\gamma = \pm(\delta \pm \frac{1}{2}J_\perp)$ are the lines of quantum phase transitions (gaplessness).

TABLE I. Order parameters in terms of dual and original spins, winding numbers, number of the Majorana zero-energy edge modes N_M for nine phases of the staggered ladder shown in Fig. 3.

Region	τ order (odd sector)	μ order (even sector)	σ order	N_w	N_M
A	$\langle\tau_x\rangle$	$\langle\mu_y\rangle$	$\mathcal{O}_{z,3}$	0	4
B	$\langle\tau_x\rangle$	$\mathcal{O}_{z,\mu}$	m_x	−1	2
C	$\langle\tau_x\rangle$	$\langle\mu_x\rangle$	$\mathcal{O}_z\|^y_x$	−2	4
D	$\mathcal{O}_{z,\tau}$	$\langle\mu_x\rangle$	m_x	−1	2
E	$\langle\tau_y\rangle$	$\langle\mu_x\rangle$	$\mathcal{O}_{z,3}$	0	4
F	$\langle\tau_y\rangle$	$\mathcal{O}_{z,\mu}$	m_y	1	2
G	$\langle\tau_y\rangle$	$\langle\mu_y\rangle$	$\mathcal{O}_z\|^x_y$	2	4
H	$\mathcal{O}_{z,\tau}$	$\langle\mu_y\rangle$	m_y	1	2
I	$\mathcal{O}_{z,\tau}$	$\mathcal{O}_{z,\mu}$	$\mathcal{O}_{z,1}$	0	0

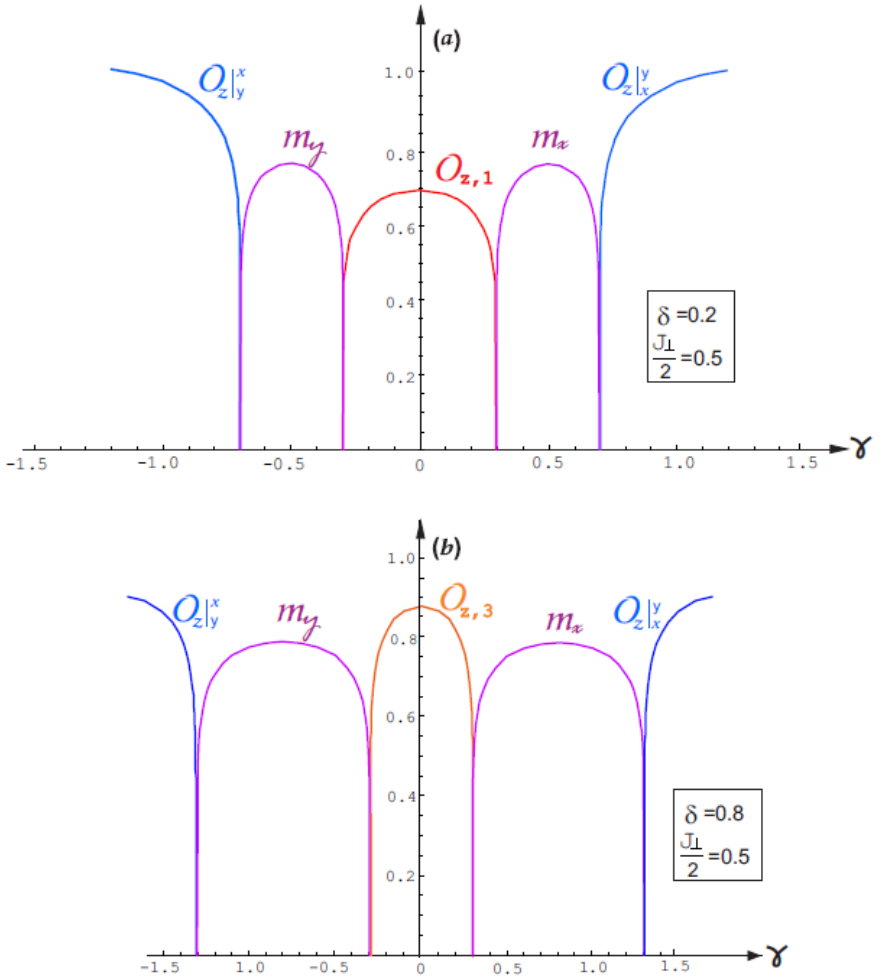

FIG. 6. Order parameters of the staggered ladder along two paths indicated in Fig. 3. (a): $\delta = 0.2$ (path 1); (b): $\delta = 0.8$ (path 2); $t = 1$ in both cases.

Fundamental properties: Phases and transitions

$Z = Tre^{-\beta H}$ ← Partition function

Pioneering papers:

C. N. Yang and T. D. Lee, Phys. Rev. **87**, 404 (1952) T. D. Lee and C. N. Yang, *ibid.* **87**, 410 (1952)

See also: K. Huang, Statistical Mechanics, 1987

$Z = 0$

Solutions for zeros of partition function in the range of **REAL** values of physical parameters

↕

1. Thermal phase transitions
2. T=0: Quantum phase transitions, zeroes of spectrum (eigenvalues of H)

Solutions for zeros of partition function in the range of **COMPLEX** values of physical parameters

↕

Disorder lines, aka modulation transitions, disentanglement

J. Stephenson, Can. J. Phys. **48**, 1724 (1970), *ibid* **48**, 2118 (1970); Phys. Rev. B **1**, 4405 (1970).

P.N. Timonin and G.Y.C., PRB 104, 045106 (2021)
P.N. Timonin and G.Y.C., PRE **96,** 062123 (2017)

NB: No information about order parameter or symmetry (breaking) is required.

$$H_{MF} = \frac{1}{2}\sum_n \left\{ \sum_\alpha (-1)^{n+\alpha-1} \left[J_{\alpha R}(n) c_\alpha^\dagger(n) c_\alpha(n+1) + \Gamma_R(n) c_\alpha^\dagger(n) c_\alpha^\dagger(n+1) \right] + J_{\perp R}(n) c_1^\dagger(n) c_2(n) + h.c. \right\}$$

$$Z = 0$$

$$\varepsilon(z) = i\omega_n, \quad \omega_n \equiv \pi T(2n+1)$$

Spectrum eigenvalues

T=0 limit:

$$\boldsymbol{\varepsilon(z) = 0}$$

$$\boldsymbol{z = e^{ik}}$$

$$\boldsymbol{k \in \mathbb{R}} \longrightarrow \text{Quantum phase transition}$$

$$\boldsymbol{k \in \mathbb{C}} \longrightarrow \text{Disorder line, aka modulation transition, disentanglement}$$

Winding numbers and zero-energy Majorana edge modes:

With a unitary transformation, the Hamiltonian

$$\hat{\mathcal{H}}(k) = \begin{pmatrix} \hat{A} & \hat{B} \\ \hat{B}^\dagger & -\hat{A} \end{pmatrix},$$

can be brought to the block off-diagonal form:

$$\hat{\mathcal{H}}'(k) = \begin{pmatrix} 0 & \hat{D}(k) \\ \hat{D}^\dagger(k) & 0 \end{pmatrix} \quad \hat{D}(k) \equiv \hat{A}(k) + \hat{B}(k),$$

Winding number is defined as an integral over the Brillouin zone:

$$N_w^\sharp = \frac{1}{2\pi i} \int_{-\pi/2}^{\pi/2} dk \partial_k \ln \det \hat{D}_\sharp,$$

where

$$\hat{A} \equiv \begin{pmatrix} t\cos k & J_\perp/2 \\ J_\perp/2 & -t\cos k \end{pmatrix} \qquad \hat{B}_\sharp \equiv \begin{pmatrix} -i\gamma_\sharp \sin k & 0 \\ 0 & i\gamma_\sharp \sin k \end{pmatrix}, \quad \sharp = e, o.$$

$$\gamma_{o/e} = \gamma \pm \delta$$

$$H_{\mathrm{MF}} = H_o + H_e,$$

G. Y. Chitov, K. Gadge, and P. N. Timonin,
PHYSICAL REVIEW B **106**, 125146 (2022)

Upon analytical continuation of the wave numbers onto the complex plane $e^{i2k} = z$ the winding number becomes the logarithmic residue of $\det D$:

$$N_w^{\sharp} = \oint_{|z|=1} \frac{dz}{2\pi i} \partial_z \ln \det \hat{D}_{\sharp}.$$

$$N_w = N_w^e + N_w^o,$$

The zeros of $\det \hat{D}$ are also zeros of the spectra $E_{\pm}$ of the XY chain, since $(E_+E_-)^2 = \det \hat{D}\hat{D}^{\dagger}$. Any change of winding number means that a root (roots) crossed the unit circle $|z| = 1$, which signals a quantum phase transition

$$\det \hat{D}_{\sharp}(z) = -\frac{(1-\gamma_{\sharp})^2}{4z}(z - z_+)(z - z_-),$$

where $z_{\pm}$ are the roots of the quadratic equation

$$(1-\gamma_{\sharp})^2 z^2 + 2(1 - \gamma_{\sharp}^2 + J_{\perp}^2/2)z + (1+\gamma_{\sharp})^2 = 0,$$

The important property of the roots $z_{\pm}$ is that they are also the eigenvalues of the transfer matrix which yields the wave functions of the zero-energy Majorana modes localized near the opposite ends of the dual (even or odd) chains

Number of roots inside a unit circle ⟷ total number of Majorana edge (localized) modes for each phase, see Table I.

Lee-Yang zeroes, disorder lines and disentanglement:

$$H_{\mathrm{MF}} = H_o + H_e,$$

$z_{+/-} \in \mathbb{C}, \quad z_+ = z_-^*$ ⟶ IC oscillations of the *EVEN* sector are localized at:

$$|\gamma| > |\delta \pm \sqrt{t^2 + J_\perp^2/4}|.$$

IC oscillations of the *ODD* sector are localized at:

$$|\gamma| > |-\delta \pm \sqrt{t^2 + J_\perp^2/4}|.$$

The wave numbers of IC oscillations are defined in the reciprocal space of the dual even/odd chains. They are:

$$q_\sharp = \arcsin \frac{J_\perp}{2\sqrt{\gamma_\sharp^2 - t^2}},$$

where $q_\sharp$ evolves smoothly from $\pi/2$ on the DL to $q_\sharp \to 0$ when $\gamma_\sharp \to \infty$.

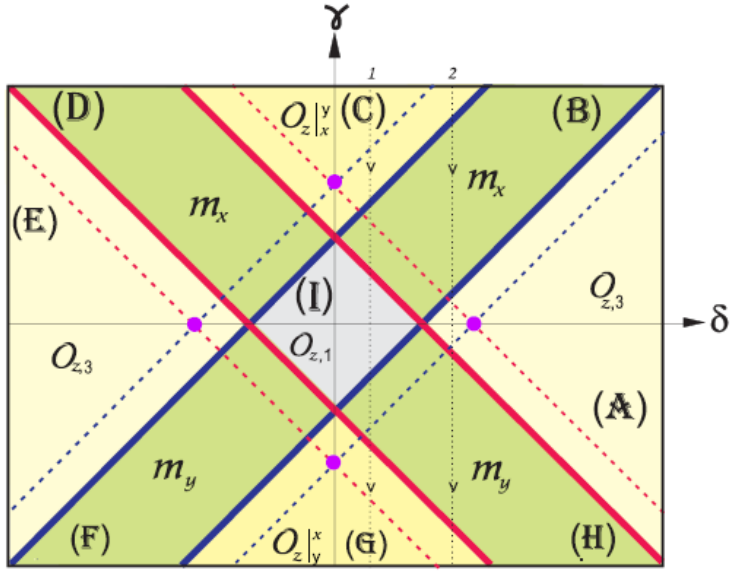

FIG. 3. Phase diagram of the anisotropic staggered two-leg ladder. Nonvanishing brane and local order parameters are shown in nine regions (A–I) of the (δ, γ) parametric plane. The solid bold blue/red lines $(\gamma \mp \delta)^2 = J_\perp^2/4$ are the lines of quantum phase transitions (phase boundaries). The dashed blue/red lines denote the even/odd disorder lines $(\gamma \mp \delta)^2 = t^2 + J_\perp^2/4$ which are bounds of the IC modulations in the even/odd sectors of the Hamiltonian, respectively. The bold magenta dots are the points of disentanglement with the factorized ground state of the Hamiltonian.

$$H_{\mathrm{MF}} = H_o + H_e, \longrightarrow |GS\rangle = |GS_e\rangle \otimes |GS_o\rangle.$$

EVEN/ODD DLs ⟷ Factorized EVEN/ODD sectors of the GS (partial disentanglement)

$$|GS_\sharp\rangle = \prod_{n=1}^{N} (\cos\vartheta_\sharp\,|\uparrow\rangle_{2n/2n-1} + \sin\vartheta_\sharp\,|\downarrow\rangle_{2n/2n-1}),$$

where the even/odd parametric angles $\vartheta_\sharp$ are defined via the following equation:

$$\cos^2 2\vartheta_\sharp = \frac{|\gamma_\sharp| - t}{|\gamma_\sharp| + t}.$$

EVEN/ODD DLs cross ⟷ Factorized GS (disentanglement)

$$\mathfrak{D}_{zz}(2, 2n+1) = \pm \sin^2 2\vartheta_e \sin^2 2\vartheta_o = \pm\left(\frac{2t}{\delta + t}\right)^2$$

$$\mathcal{C} = \mathcal{E} = 0.$$

→ EVEN/ODD correlators are CONSTANT on their corresponding DLs. For instance: *(Region A)*

$$\mathfrak{D}_{xx}(2, 2n+1) = \pm \sin^2 2\vartheta_o, \ \forall n.$$

$$\mathfrak{D}_{yy}(2, 2n+1) = \pm \sin^2 2\vartheta_e, \ \forall n.$$

Concurrence and global entanglement:

$$\text{even/odd DLs} : \mathcal{C}, \mathcal{E} \mapsto \min.$$

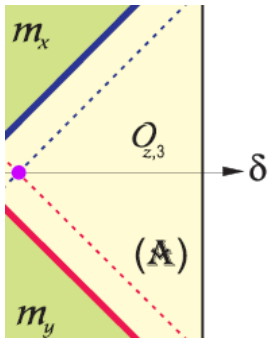

Columnar ladder:

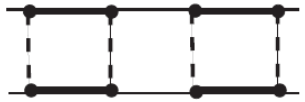

$$H_{\rm MF} = H_o + H_e,$$

$$H_o = \frac{1}{4}\sum_{l=1}^{N}\{(t-(-1)^l\delta+\gamma)\tau^x_{2l-1}\tau^x_{2l+1} + (t-(-1)^l\delta-\gamma)\tau^y_{2l-1}\tau^y_{2l+1} + (-1)^l J_\perp \tau^z_{2l-1}\},$$

$$H_e = \frac{1}{4}\sum_{l=1}^{N}\{(t-(-1)^l\delta+\gamma)\mu^x_{2l-2}\mu^x_{2l} + (t-(-1)^l\delta-\gamma)\mu^y_{2l-2}\mu^y_{2l} + (-1)^l J_\perp \mu^z_{2l-2}\}.$$

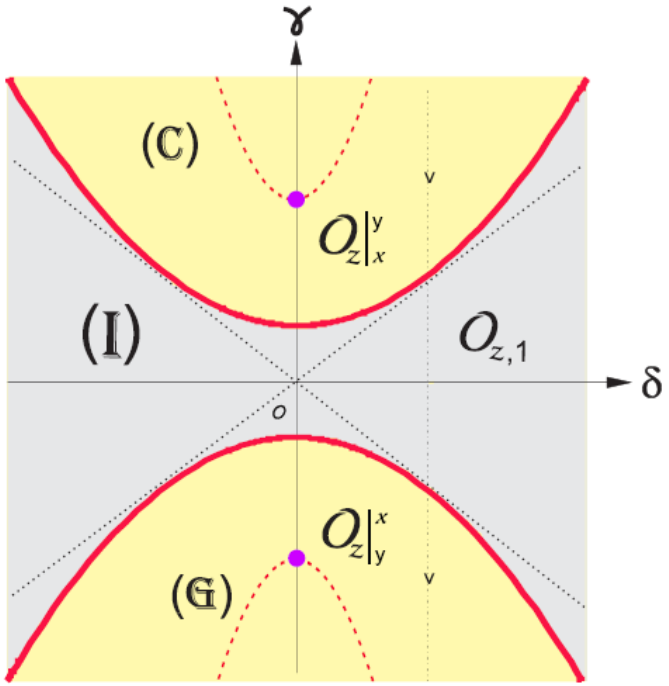

FIG. 4. Phase diagram of the anisotropic columnar two-leg ladder. Nonvanishing brane order parameters are shown in three regions C, G, and I on the (δ, γ) parametric plane. The bold red lines $\gamma^2 = \delta^2 + J_\perp^2/4$ are the lines of quantum phase transitions. The dashed red lines denote the disorder lines $\gamma^2 = (1 + 4t^2/J_\perp^2)(\delta^2 + J_\perp^2/4)$ bounding the IC modulations. The bold magenta dots are the points of disentanglement with the factorized ground state of the Hamiltonian.

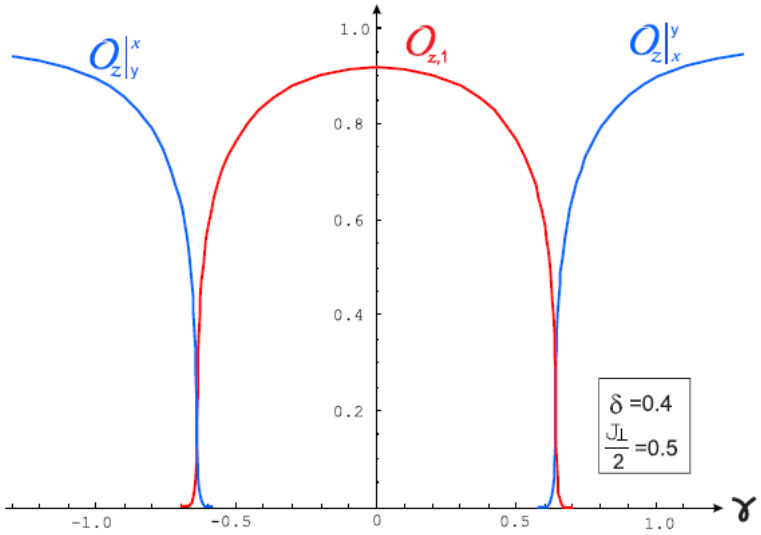

FIG. 7. Brane order parameters in the columnar ladder along the path indicated in Fig. 4. The tails seen near the critical points are finite-size effects: the results are obtained numerically from 140 × 140 Toeplitz matrices.

Order Parameter Calculations:

The spin-correlation function can be calculated as the correlation function of the Majorana string operators

$$\langle \sigma_L^x \sigma_R^x \rangle = \langle O_x(L) O_x(R) \rangle = \left\langle \prod_{n=L}^{R-1} [i b_n a_{n+1}] \right\rangle.$$

Majorana correlation function, found analytically

$$\langle i b_n a_m \rangle = \frac{1}{2\pi} \int_{-\pi}^{\pi} dq e^{-iq(m-n)} \{ G_{11}(q) + (-1)^n G_{12}(q) \},$$

The latter is given by the determinant:

$$\langle \sigma_L^x \sigma_R^x \rangle = \begin{vmatrix} \langle i b_L a_{L+1} \rangle & \langle i b_L a_{L+2} \rangle & \dots & \langle i b_L a_R \rangle \\ \langle i b_{L+1} a_{L+1} \rangle & \langle i b_{L+1} a_{L+2} \rangle & \dots & \langle i b_{L+1} a_R \rangle \\ \vdots & \ddots & \ddots & \vdots \\ \langle i b_{R-1} a_{L+1} \rangle & \langle i b_{R-1} a_{L+2} \rangle & \dots & \langle i b_{R-1} a_R \rangle \end{vmatrix}.$$

Toeplitz block determinants

string correlation function:

$$\mathfrak{D}_{zz}(L,R) \equiv \langle O_z(L-1) O_z(R) \rangle = \left\langle \prod_{l=L}^{R} [i b_l a_l] \right\rangle = \begin{vmatrix} \langle i b_L a_L \rangle & \langle i b_L a_{L+1} \rangle & \dots & \langle i b_L a_R \rangle \\ \langle i b_{L+1} a_L \rangle & \langle i b_{L+1} a_{L+1} \rangle & \dots & \langle i b_{L+1} a_R \rangle \\ \vdots & \ddots & \ddots & \vdots \\ \langle i b_R a_L \rangle & \langle i b_R a_{L+1} \rangle & \dots & \langle i b_R a_R \rangle \end{vmatrix}.$$

Experiments to detect the brane order:

Observation of a Spin Gap in $SrCu_2O_3$ Comprising Spin-$\frac{1}{2}$ Quasi-1D Two-Leg Ladders

M. Azuma, Z. Hiroi, and M. Takano
Institute for Chemical Research, Kyoto University, Uji, Kyoto-fu 611, Japan

K. Ishida and Y. Kitaoka
Department of Material Physics, Faculty of Engineering Science, Osaka University, Toyonaka, Osaka-fu 560, Japan
(Received 24 June 1994)

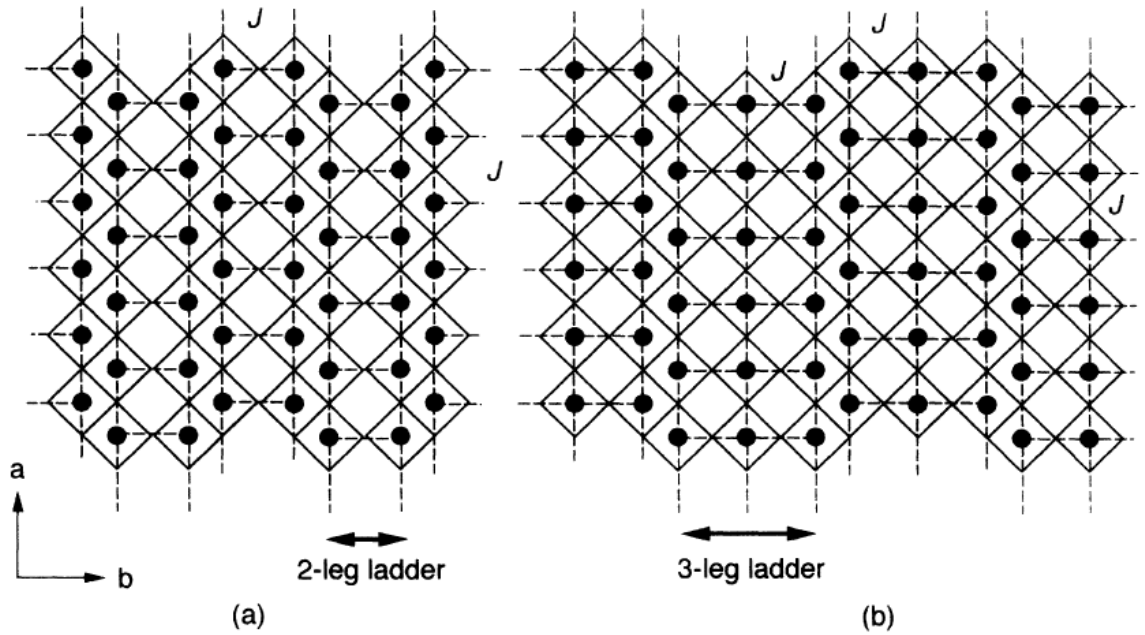

FIG. 1. Schematic drawings of the Cu_2O_3 sheet of $SrCu_2O_3$ (a) and the Cu_3O_5 sheet of $Sr_2Cu_3O_5$ (b). The filled circles are Cu^{2+} ions, and O^{2-} ions exist at the corners of the squares drawn with solid lines. Cu spins are strongly coupled with each other via an essentially uniform antiferromagnetic exchange within each ladder, while the ladders are separated from each other in effect because of the weakness of the exchange interaction via the 90° Cu-O-Cu bond plus the spin frustration due to symmetry at the interface.

$SrCu_2O_3$

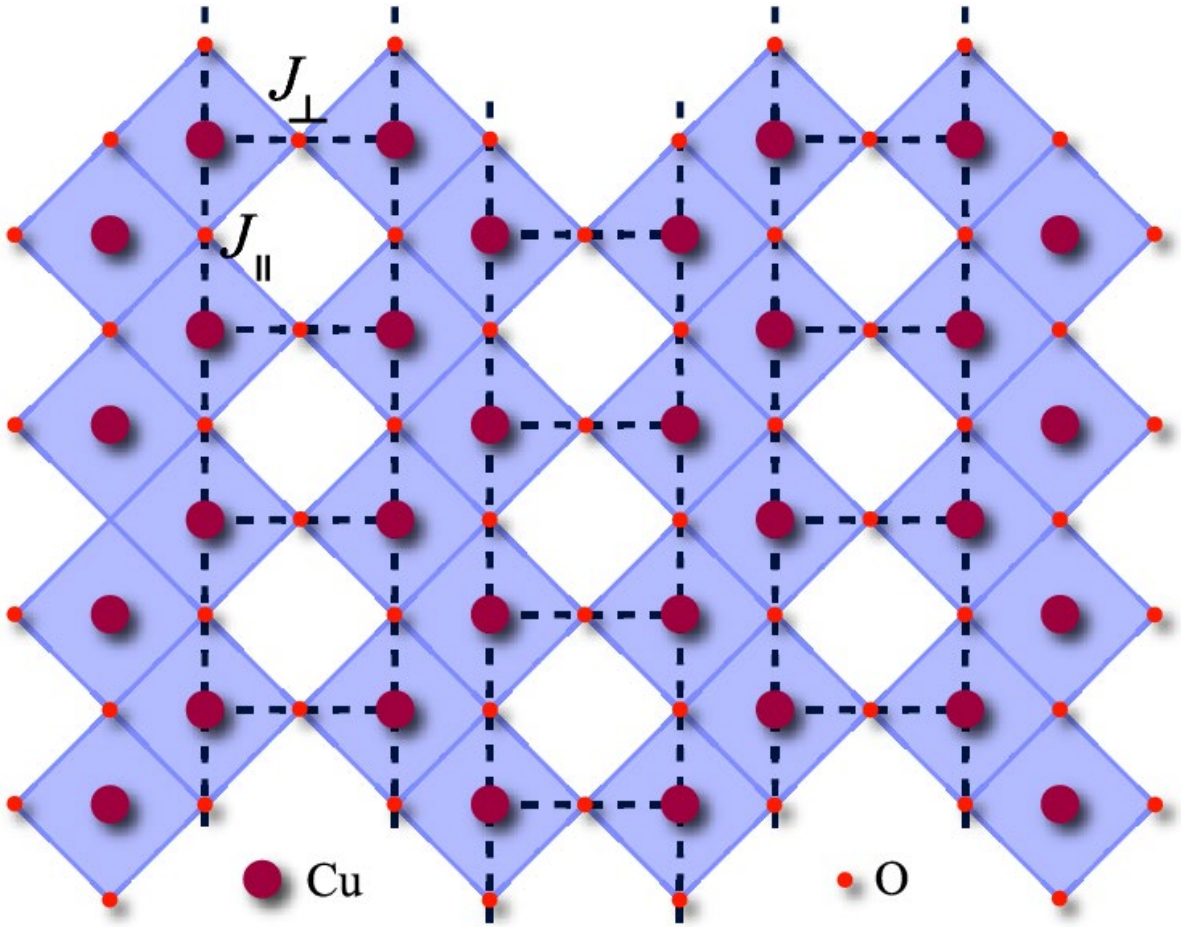

Realizing the symmetry-protected Haldane phase in Fermi–Hubbard ladders

Pimonpan Sompet[1,2,3,10]✉, Sarah Hirthe[1,2,10], Dominik Bourgund[1,2,10], Thomas Chalopin[1,2], Julian Bibo[2,4], Joannis Koepsell[1,2], Petar Bojović[1,2], Ruben Verresen[5], Frank Pollmann[2,4], Guillaume Salomon[1,2,6,7], Christian Gross[1,2,8], Timon A. Hilker[1,2] & Immanuel Bloch[1,2,9]✉

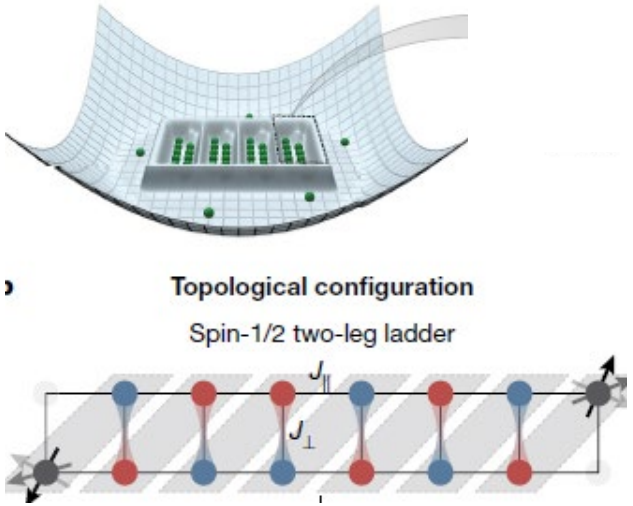

Fig. 1 | Probing topological phases in spin-1/2 ladders of cold atoms. **a**, Realization of tailored spin-1/2 ladders in a single plane of a 3D optical lattice

spin ladder realizes the Heisenberg model[28] with Hamiltonian:

$$\hat{H} = J_\parallel \sum_{\substack{x\in[0,L) \\ y=A,B}} \hat{\mathbf{S}}_{x,y}\cdot\hat{\mathbf{S}}_{x+1,y} + J_\perp \sum_{x\in[0,L)} \hat{\mathbf{S}}_{x,A}\cdot\hat{\mathbf{S}}_{x,B} \qquad (1)$$

with positive leg and rung couplings, $J_{\parallel,\perp} = 4t_{\parallel,\perp}^2/U$ and the spin-1/2 operators $\hat{\mathbf{S}}_{x,y}$ at site (x,y), with A, B denoting the two legs of the ladder.

Observation of brane parity order in programmable optical lattices

David Wei,[1,2] Daniel Adler,[1,2] Kritsana Srakaew,[1,2] Suchita Agrawal,[1,2]
Pascal Weckesser,[1,2] Immanuel Bloch,[1,2,3] and Johannes Zeiher[1,2]

arXiv:2301.11869

In our experiment, we worked with about 200 ^{87}Rb atoms in the $|F = 1, m_F = -1\rangle$ ground state, trapped in lattices at a wavelength of $\lambda = 1064\,\text{nm}$ and with DMD block-out beams operating at 670 nm

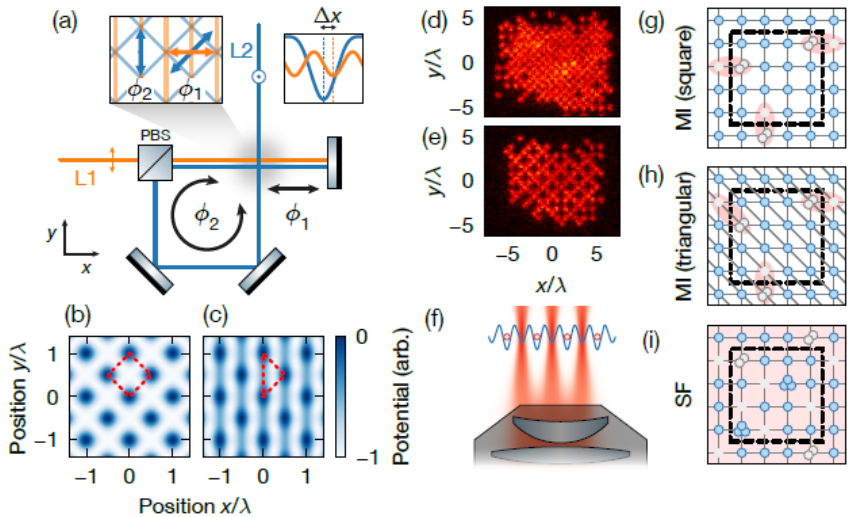

FIG. 1. (a) Experimental setup realizing passively phase-stable tunable lattices

The Bose-Hubbard model is given by

$$\hat{H} = -\sum_{\langle i,j \rangle} J_{ij} \hat{c}_i^\dagger \hat{c}_j + \frac{U}{2} \sum_i \hat{n}_i (\hat{n}_i - 1) + \sum_i V_i \hat{n}_i .$$

Parity brane (string) order parameter is defined in the limit $D \to \infty$

$$\langle \mathcal{O}^2(\mathcal{D}) \rangle = \left\langle e^{i\pi \sum_{i \in \mathcal{D}} (\hat{n}_i - \bar{n})} \right\rangle = \left\langle \prod_{i \in \mathcal{D}} (-1)^{\bar{n}} \hat{p}_i \right\rangle, \tag{3}$$

where $\mathcal{D}$ is a spatial domain, i.e., an interval in $d = 1$ and an area in $d = 2$, and $\hat{p}_i = (-1)^{\hat{n}_i}$ is the parity operator on lattice site i.

S.P. Rath et al. / Annals of Physics 334 (2013) 256–271

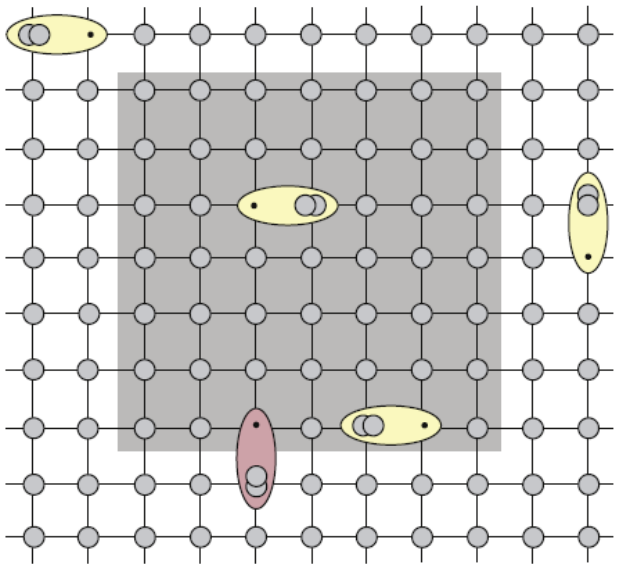

Experimental observations:

1. M. Enders, *et al*, Science **334**, 200 (2011);
2. S. de Leseleuc, *et al*, Science **365**, 775 (2019);
3. P. Sompet, *et al*, Nature, **606**, 484 (2022);
4. C.K. Thomas, *et al*, PRL **119**, 100402 (2017);
5. D. Wei, *et al*, arXiv:2301.11869.

"*Обобщенная теория фазовых переходов в низкоразмерных системах с нелокальным (топологическим) упорядочением*".

Pertinent papers (15):

Group I: ladders, interacting models

(Ia). T. Pandey and G.Y. Chitov, *Brane order and quantum magnetism in modulated anisotropic ladders*, Phys. Rev. B **106**, 094413, 17 pages (2022).

(Ib). G.Y. Chitov and T. Pandey, *Constructing Landau Framework for Topological Order: Quantum Chains and Ladders*, J. Stat. Mech. (2017) 043101, 25 pages.

(Ic). S.J. Gibson, R. Meyer, G.Y. Chitov, *Numerical Study of Critical Properties and Hidden Orders in Dimerized Spin Ladders*, Phys. Rev. B **83**, 104423, 7 pages (2011).

(Id). G.Y. Chitov, B.W. Ramakko, M. Azzouz, *Quantum Criticality in Dimerized Spin Ladders*, Phys. Rev. B **77**, 224433, 7 pages (2008).

(Ie). M. Azzouz, K. Shahin, G.Y. Chitov, *Spin-Peierls Instability in the Three-Leg Heisenberg Ladder*, Phys. Rev. B **76**, 132410, 4 pages (2007).

Group II: chains, free and interacting models

(IIa). G.Y. Chitov, *Local and nonlocal order parameters in the Kitaev chain*, Phys. Rev. B **97**, 085131, 7 pages (2018).

(IIb). G.Y. Chitov, T. Pandey, and P.N. Timonin, *String and conventional order parameters in the solvable modulated quantum chain*, Phys. Rev. B **100**, 104428, 12 pages (2019).

(IIc). T. Pandey and G.Y. Chitov, *Phase diagram and topological order in the modulated XYZ chain with magnetic fields*, Phys. Rev. B **102**, 054436, 16 pages (2020).

Group III: disorder lines (modulation transitions), Lee-Yang zeros, disentanglement

(IIIa). P.N. Timonin and G.Y. Chitov, *Infinite cascades of phase transitions in the classical Ising chain*, Phys. Rev. E **96**, 062123, 7 pages (2017).

(IIIb). P.N. Timonin and G.Y. Chitov, *Disorder lines, modulation, and partition function zeros in free fermion models*, Phys. Rev. B **104**, 045106, 12 pages (2021).

(IIIc). G.Y. Chitov, K. Gadge, and P.N. Timonin, *Disentanglement, disorder lines, and Majorana edge states in a solvable quantum chain*, Phys. Rev. B **106**, 125146, 14 pages (2022).

Group IV: cascades of geometric transitions

(IVa). P.N. Timonin and G.Y. Chitov, *Hidden Percolation Transition in Kinetic Replication Process*, J. Phys. A: Math. Theor. **48**, 135003, 18 pages (2015).

(IVb). P.N. Timonin and G.Y. Chitov, *Exploring Percolative Landscapes: Infinite Cascades of Geometric Phase Transitions*, Phys. Rev. E **93**, 012102, 10 pages (2016).

Group V: IC/floating phase (BKT transition) in 2D Ising model

(Va). G.Y. Chitov and C. Gros, *Ordering in Two-Dimensional Ising Models with Competing Interactions*, Low Temperature Physics **31**, 722-734 (2005) [Fizika Nizkikh Temperatur **31**, 952-967 (2005)].

(Vb). A. Kalz and G.Y. Chitov, *Topological Floating Phase in a Spatially Anisotropic Frustrated Ising Model*, Phys. Rev. B **88**, 014415, 9 pages (2013).

THE END

THANK YOU!